Original Article

Molecular typing, antibiotic susceptibility, and biofilm production in nonencapsulated *Streptococcus pneumoniae* isolated from children in Japan[☆]

Noriko Takeuchi [a, *], Misako Ohkusu [a], Noriyuki Wada [b], Satoko Kurosawa [c], Akiko Miyabe [d], Masashi Yamaguchi [e], Moon H. Nahm [f], Naruhiko Ishiwada [a]

[a] Department of Infectious Diseases, Medical Mycology Research Center, Chiba University, Chiba, Japan
[b] Wada Pediatric Clinic, Tokyo, Japan
[c] Kurosawa Children's and Internal Medicine Clinic, Tokyo, Japan
[d] Division of Laboratory Medicine and Clinical Genetics, Chiba University Hospital, Chiba, Japan
[e] Medical Mycology Research Center, Chiba University, Chiba, Japan
[f] Division of Pulmonary, Allergy & Critical Care Medicine, Department of Medicine, The University of Alabama at Birmingham, Birmingham, AL, USA

ARTICLE INFO

ABSTRACT

The prevalence of nonencapsulated *Streptococcus pneumoniae* (NESp) has increased with the introduction of pneumococcal conjugate vaccines in children; however, the bacteriological characteristics of NESp have not been sufficiently clarified. In this study, NESp strains isolated from the nasopharyngeal carriage of children from four nursery schools in Japan were analyzed for molecular type, antibiotic susceptibility, and biofilm productivity. A total of 152 putative *S. pneumoniae* strains were identified by optochin-susceptibility analysis, of which 21 were not serotypeable by slide agglutination, quellung reaction, or multiplex PCR. Among these 21 strains, three were *lytA*-negative and, therefore, not *S. pneumoniae*. The remaining 18 strains were positive for *lytA*, *ply*, *pspK*, and bile solubility and were confirmed as NESp. Therefore, the isolation rate of NESp in the *S. pneumoniae* strains in this study was 12.0% (18/149). Molecular-typing analyses classified five strains as two existing sequence types (STs; ST7502 and ST7786), and 13 strains formed four novel STs. Horizontal spread was suspected, because strains with the same ST were often isolated from the same nursery school. The NESp isolates were generally susceptible to most antimicrobials, with the exception of macrolides; however, all isolates possessed more than one abnormal penicillin-binding protein gene. Furthermore, NESp strains were more effective than encapsulated counterparts at forming biofilms, which showed obvious differences in morphology. These data indicated that NESp strains should be continuously monitored as emerging respiratory pathogens.

© 2019 Japanese Society of Chemotherapy and The Japanese Association for Infectious Diseases. Published by Elsevier Ltd. All rights reserved.

1. Introduction

Streptococcus pneumoniae colonizes the upper respiratory tract and can be a major causal pathogen of otitis media, pneumonia, and invasive diseases, such as sepsis and meningitis, in children. More than 95 different polysaccharide capsule (CPS) types have been identified. The increased use of the pneumococcal conjugate vaccine (PCV) in infants has decreased the total number of invasive pneumococcal disease (IPD) cases; however, the percentage of those caused by non-vaccine serotypes has increased dramatically, suggesting that non-vaccine serotype IPDs have replaced vaccine serotype IPDs [1–3]. A similar change has also been observed in *S. pneumoniae* isolated from nasopharyngeal carriage [4]. Most *S. pneumoniae* are regarded as harboring a CPS; however, the existence of nonencapsulated *S. pneumoniae* (NESp) was recently reported. NESp is mainly classified into two types based on CPS presence. The first group harbors a non-functional capsular polysaccharide synthesis (*cps*) locus located between the glucan 1,6-a-

glucosidase gene (*dexB*) and the oligopeptide ABC-transporter gene (*aliA*). Previous studies found that *cps* becomes non-functional because of mutations in the initiating glucose phosphate trans-ferase (*cpsE*; also identified as *wchA*) [5,6]. These strains are non-typeable with the quellung reaction using pneumococcal antisera, but can be typed by PCR. The second group comprises true NESp that completely lacks the *cps* locus, which is replaced with other gene sequences. The lack of the capsular polysaccharide biosyn-thesis gene (*cpsA*; also identified as *wzg*) identifies this group, which is divided into four clades based on the presence of three genes encoding pneumococcal surface protein K (*pspK*; also iden-tified as *nspA*) and two oligopeptide-binding lipoproteins (*aliB*-like homologs called *aliC* and *aliD*). These four groups are named null-capsule clade (NCC)1, NCC2, NCC3, and NCC4 [6−8]. NCC1 harbors the gene encoding the virulence factor *pspK*, which possesses basic structure and size variations and is negative for *aliC* and *aliD* [7−10]. NCC2 is *aliC*- and *aliD*-positive, but negative for *pspK*, and NCC3 is *aliD*-positive, but negative for *aliC* and *pspK*. NCC4 contains only transposable elements in the *cps* locus.

For the clinical aspects of NESp, a recent study reported that the NESp rate was 12.5% for streptococcal carriage in children [11]. Because PCVs do not provide immunity against NESp, the appear-ance of NESp might be related to the wide use of PCVs for children. Additionally, NESp pathogenicity has not been clarified, with pre-vious reports indicating that NESp rarely cause IPD [1]. On the other hand, NESp induces non-invasive diseases, such as otitis media, sinusitis, and conjunctivitis [11−14], and it is expected that respi-ratory infections caused by NESp will increase along with increases in the NESp carriage rate in children. Therefore, understanding NESp pathogenicity and drug sensitivity is critically important to formulate effective treatment strategies.

In this study, we characterized NESp strains by multi-locus sequence typing (MLST) and assessed strains for *cps* and *pspK* expression. Additionally, we examined drug sensitivity, mutations in genes encoding penicillin-binding proteins (PBPs), and the presence of macrolide- and quinolone-resistance genes. Moreover, we determined differences in biofilm formation between typeable *S. pneumoniae* and NESp strains by microtiter biofilm assays (MBAs) and scanning electron microscopy (SEM).

2. Materials and methods

2.1. S. pneumoniae strains

S. pneumoniae strains were isolated from nasopharyngeal or nasal-swab specimens collected from healthy children (0−1-years old) who were newly enrolled into four nursery schools in Tokyo, Japan, from October 2012 to March 2015. The three nursery schools (A,B,C) are located in the same region, east of Tokyo, and the other one (D) is located in a different region, west of Tokyo. The two re-gions are approximately 30 km apart in straight-line distance. Parents provided written informed consent, and this study was approved by the Ethical Committee of Medical Mycology Research Center, Chiba University (Permission No. 2017−12). There were 11 targeted children in 2012, 39 in 2013, and 37 in 2014. There were no duplicate specimens for children enrolled in 2012; however, in 2013 and 2014, specimens were collected three times per child per year in general (April−June, September−November, Januar-y−March), the total number of specimens was 231. In total, 152 nasopharyngeal carriage isolates were identified by optochin-susceptibility test and were stored in 10% skim milk at −80 °C until analysis. Isolates were propagated on trypticase soy agar (TSA) with 5% sheep blood (Nippon Becton Dickinson Co. Ltd., Tokyo, Japan) and Todd-Hewitt broth plus 0.5% yeast extract (THYB) for 18 h at 37 °C in 5% CO_2. Bacterial genomic DNA was extracted using

a MORA-EXTRACT kit (Kyokuto Pharmaceuticals, Tokyo, Japan) and stored at −20 °C. Isolates were serotyped by slide agglutination reactions with the *S. pneumoniae* antisera ('Seiken' set; Denka Seiken, Tokyo, Japan), quellung reactions with pneumococcal antisera (Statens Serum Institute, Copenhagen, Denmark), and multiplex PCR [15]. Further characterization was performed by bile solubility testing and PCR analysis for pneumococcal autolysin (*lytA*) and the intracellular toxin pneumolysin (*ply*). Polysaccharide cell-wall composition was also assessed using ~10^8 CFU/mL bacte-rial solution and three rapid antigen-detection kits [BinaxNOW pneumococcal antigen kit (Alere, Inc., Waltham, MA, USA); RAP-IRUN *S. pneumoniae* and RAPIRUN *S. pneumoniae* HS (Otsuka Pharmaceutical Co. Ltd., Tokyo, Japan)] [16,17].

2.2. Analysis of capsule-phase variants and molecular typing

Presence of *cpsA*, *pspk*, *aliC*, and *aliD* was determined by PCR amplification as previously described [7]. The PCR products were purified with FastGene Gel/PCR extraction kit (NIPPON Genetics, Tokyo, Japan) and subjected to sequence analysis with a Big Dye Terminator version 3.1 cycle sequencing kit on an Applied Bio-systems 3130xl genetic analyzer (Applied Biosystems, Foster City, CA, USA). The repeat number of the α-helical repeat structure A(E)(E)EEA/TKR/QK contained in *pspK* was counted, and the *pspk* sequences of all strains were registered in GenBank (accession numbers LC258112−LC258129).

MLST was used to analyze seven housekeeping genes (*aroE*, *gdh*, *gki*, *recP*, *spi*, *xpt*, and *ddl*) by PCR, as previously described [18]. PCR products were purified with a FastGene Gel/PCR extraction kit (NIPPON Genetics) and subjected to sequence analysis with a Big Dye Terminator version 3.1 cycle sequencing kit on an Applied Biosystems 3130xl genetic analyzer (Applied Biosystems). Allelic numbers and sequence types (STs) were determined using an MLST database (https://pubmlst.org/spneumoniae/).

The relatedness of the isolates was determined by constructing a gene tree with the neighbor-joining method using MEGA7.

2.3. Antimicrobial susceptibility and drug-resistance gene analysis

Antimicrobial-susceptibility testing was performed by broth microdilution according to guidelines of the Clinical and Laboratory Standards Institute (for 22 h at 35 °C in ambient air) to determine minimum inhibitory concentration (MIC). *S. pneumoniae* ATCC 49619 was used as reference strain for the antibiotic susceptibility test. Three strains were not grown in ambient air, but rather under 5% CO_2 for the antibiotic susceptibility test. Antimicrobial agents employed in this study included penicillin G (PEN), cefotaxime (CTX), imipenem (IPM), clarithromycin (CLR), clindamycin (CLI), vancomycin (VAN), tosufloxacin (TFX), and levofloxacin (LVX). The MIC breakpoints for TFX were determined according to recom-mendations for respiratory infections established by the Japanese Society of Chemotherapy [19].

Mutations in genes encoding penicillin-binding proteins (i.e., *pbp1a*, *pbp2x,* and *pbp2b*) and the presence of the macrolide-resistance genes *mef*(A) and *erm*(B) were assessed by PCR with the penicillin-resistant *S. pneumoniae* detection reagent kit (Wakunaga Pharmaceutical, Osaka, Japan). The quinolone resistance-determining regions (QRDRs) of gyrase (*gyr*)A, *gyrB*, *parC*, and *parE* were amplified and sequenced as described previously [20].

2.4. In vitro biofilm-formation assays

Biofilm formation was assessed by microtiter biofilm assay (MBA). To compare NESp strains with encapsulated strains, encapsulated strains were isolated from nasopharyngeal carriage

and from otorrhea or middle-ear effusion with acute otitis media (AOM). Isolates were precultured on TSA in 5% sheep blood at 37 °C in 5% CO_2 for 24 h, followed by isolation of single colonies, which were subcultured on the same medium. On the third day, cultures were transferred to THYB overnight, and 5 μL of the bacterial solution ($OD_{600} = 0.15-0.65$) was added to the wells of 96-well polystyrene microplates (AS ONE Corporation, Osaka, Japan) along with 200 μL THYB and incubated for 18 h at 37 °C under 5% CO_2 overnight. Plates were washed three times with water, stained with 100 μL of 0.5% crystal violet for 5 min, and washed another three times. After drying, 200 μL of 95% ethanol was added to each well, and absorbance at 570 nm was measured with Sunrise™ microplate reader (Tecan Japan Co. Ltd., Kanagawa, Japan). The pspK-deletion mutant MNZ1131 (derived from wild-type MNZ11 and belonging to NCC1) served as a control [7,21].

2.5. Scanning electron microscopy (SEM)

The morphology of biofilms produced by strains 15P200 (NESp strain) and 15P255 (serotype 24F) was examined by SEM, as previously described [22]. A 1 × 1.5-cm polystyrene slide was placed in a culture dish, and cells were cultured in THYB for 18 h at 37 °C in 5% CO_2. Specimens were fixed with 2.5% glutaraldehyde, post-fixed with 1% OsO_4, dehydrated with graded ethanol, and transferred with t-butyl alcohol. The samples were freeze-dried with a VFD-21S t-butyl alcohol freeze-drying apparatus (Vacuum Device Co. Ltd., Mito, Japan), coated with platinum-palladium with an E−102 ion spatter (Hitachi High Technologies, Tokyo, Japan), and observed under an S-3400 N scanning electron microscope (Hitachi High Technologies, Tokyo, Japan) at 10 kV.

2.6. Statistical analysis

Statistical analysis was performed using JMP software (v7 for Windows; https://www.jmp.com/en_us/home.html). The Mann-Whitney U test was used to analyze differences among diagnostic groups.

3. Results

3.1. S. pneumoniae strains

In total, 152 presumptive S. pneumoniae strains were detected in the nasopharyngeal carriage isolates by optochin-susceptibility testing. Twenty-one strains were nontypeable by slide agglutination and quellung reactions, and of these, 18 strains were positive for lytA and the intracellular toxin ply expression and bile solubility, indicative of S. pneumoniae. The remaining three strains were lytA-negative, and one was also bile-insoluble and, therefore, not S. pneumoniae and excluded from further analyses. All 18 nontypeable strains were confirmed as S. pneumoniae according to three rapid antigen-detection kits.

3.2. Analysis of capsule-phase variants and molecular typing

Table 1 shows the number of NESp strains among 149 isolates based on the nursery school and survey year. Eighteen NESp strains (12.0%) among 149 isolates were cpsA-negative, and all NESp strains expressed pspK, which contained 11 to 33 repeats of the α-helical repeat structure A(E)(E)EEA/TKR/QK that contained the novel repeat regions AEEEEAKRK and AEEETKQK (Table 2). GenBank accession numbers of each strain are shown in Table 2. All NESp strains were negative for both aliC and aliD, and based on this finding, all 18 strains were classified as NCC1. Additionally, MLST analysis classified the isolates into six STs (Table 3). Five

Table 1
The number of nonencapsulated strains among 149 nasopharyngeal carriage isolates of S. pneumoniae.

survey year	Nursery school (nonencapsulated strains/total)				Total (%)
	A	B	C	D	
2012.10—2013.3	0/2	0/0	0/1	0/5	0/8 (0.0)
2013.4—2014.3	3/11	3/21	0/18	0/21	6/71 (8.4)
2014.4—2015.3	0/12	2/12	4/10	6/36	12/70 (17.1)
					18/149 (12.0)

strains were classified as either ST7502 or ST7786, whereas the remaining 13 strains were classified into four new STs. ST11973, ST11974, and ST11975 consisted of known allelic profiles, whereas ST11976 contains the new allelic profile in aroE. ST7786, ST7502, ST11975, and ST11976 belonged to clonal complex (CC) 7786, and ST11974 belonged to CC1106. CC1106 strains registered in the MLST database were all nontypeable or of serotype 14, whereas ST11973 was a singleton. Fig. 1 shows the neighbor-joining tree based on the pspk gene and the concatenation of seven selected MLST fragments.

3.3. Antimicrobial-susceptibility testing and detection of drug-resistance genes

Table 4 shows the results of antimicrobial-susceptibility testing and drug-resistance genes, as well as MIC values for seven antimicrobial agents. TFX is an oral fluoroquinolone released for children in January 2010 in Japan. To determine MICs according to antimicrobial-susceptibility testing by broth microdilution, strains were cultured at 35 °C in ambient air, whereas strains 15P291, 15P292, and 15P293 were grown under 5% CO_2.

Four strains showed reduced susceptibility to PEN (0.12—0.25 mg/L), and 11 strains showed resistance to CLR (≥1 mg/L). The MICs of IPM, TFX, and LVX for all strains each showed susceptibility at ≤0.06 mg/L, ≤0.12 mg/L, and ≤2 mg/L, respectively. All strains possessed at least one mutation in a PBP, with PBP mutations varying between STs. With respect to macrolide-resistant gene expression, all strains were positive for erm(B), whereas only the two ST7502 strains were mef(A)-positive. For quinolone resistance, the QRDRs of DNA gyrase (gyrA and gyrB) and topoisomerase IV (parC and parE) were amplified and sequenced, with multiple mutations detected. Six strains harbored a Lys137→Asn mutation in ParC, and 16 strains harbored an Ile460→Val mutations in ParE. No strains harbored mutations in gyrA or gyrB, and no strains harbored mutations in both the QRDRs of gyrA and parC related to high levels of quinolone resistance.

3.4. In vitro biofilm formation

Biofilm formation by the NESp isolates was examined by MBA (Fig. S1A). The MBA value of MNZ1131 was high, similar to that for other NESp strains. Fig. S1B shows encapsulated strains isolated from nasopharyngeal carriage, and Fig. S1C shows encapsulated strains isolated from otorrhea or middle-ear effusion with AOM. Notably, NESp strains tended to be more effective in generating biofilms than encapsulated strains, regardless of the source (p < 0.001; Mann-Whitney U test) (Fig. 2).

3.5. Biofilm morphology analysis by SEM

We compared biofilm formation of the NESp strain with that of the encapsulated strain. Fig. 3 shows SEM images of the various

Table 2
Analysis of capsule phase variants of 18 nonencapsulated strains of *S. pneumoniae*.

Strain	bile solubility test	*lytA*	*ply*	*cpsA*	*pspK*	*aliC*	*aliD*	repeat number of the α-helical repeat structure	GenBank accession no.
15P223*	+	+	+	−	+	−	−	11	LC258112
15P245*	+	+	+	−	+	−	−	33	LC258113
15P246	+	+	+	−	+	−	−	11	LC258114
15P232	+	+	+	−	+	−	−	10	LC258115
15P235	+	+	+	−	+	−	−	10	LC258116
15P237	+	+	+	−	+	−	−	10	LC258117
15P286	+	+	+	−	+	−	−	9	LC258118
15P303	+	+	+	−	+	−	−	9	LC258119
15P281	+	+	+	−	+	−	−	9	LC258120
15P291	+	+	+	−	+	−	−	9	LC258121
15P292	+	+	+	−	+	−	−	9	LC258122
15P293	+	+	+	−	+	−	−	9	LC258123
15P192**	+	+	+	−	+	−	−	30	LC258124
15P195***	+	+	+	−	+	−	−	28	LC258125
15P196	+	+	+	−	+	−	−	28	LC258126
15P200**	+	+	+	−	+	−	−	27	LC258127
15P203***	+	+	+	−	+	−	−	28	LC258128
15P205	+	+	+	−	+	−	−	28	LC258129

*, **, *** are isolated from the same child.

Table 3
Molecular typing of 18 nonencapsulated strains of *S. pneumoniae*.

Strain	*aroE*	*gdh*	*gki*	*recP*	*spi*	*xpt*	*ddl*	ST	Nursery school	Detected time
15P223*	8	29	9	15	77	155	31	7786	A	2013.4
15P245*	8	29	9	15	77	155	31	7786	A	2013.9
15P246	8	29	9	15	77	155	31	7786	A	2013.9
15P232	8	29	9	15	77	155	260	11975	B	2013.9
15P235	8	29	9	15	77	155	260	11975	B	2013.9
15P237	8	29	9	15	77	155	260	11975	B	2013.9
15P286	8	29	9	15	77	155	26	7502	B	2014.9
15P303	8	29	9	15	77	155	26	7502	B	2015.1
15P281	368	29	9	15	77	155	31	11976	C	2014.9
15P291	368	29	9	15	77	155	31	11976	C	2015.1
15P292	368	29	9	15	77	155	31	11976	C	2015.1
15P293	368	29	9	15	77	155	31	11976	C	2015.1
15P192**	1	5	4	29	2	3	50	11973	D	2015.1
15P195***	8	29	41	15	17	12	31	11974	D	2015.1
15P196	8	29	41	15	17	12	31	11974	D	2015.1
15P200**	1	5	4	29	2	3	50	11973	D	2015.3
15P203***	8	29	41	15	17	12	31	11974	D	2015.3
15P205	8	29	41	15	17	12	31	11974	D	2015.3

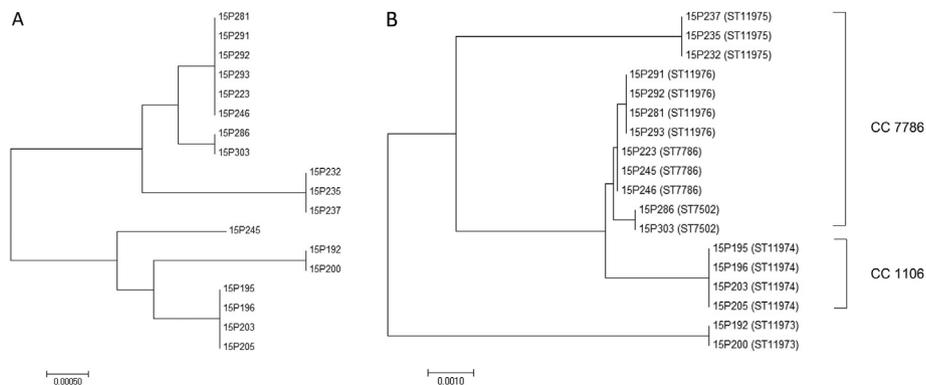*, **, *** are isolated from the same child.

Fig. 1. Neighbor-joining tree based on *pspK* fragments and the concatenation of seven selected MLST fragments. (A) Neighbor-joining tree based on *pspK* fragments. (B) Neighbor-joining tree based on the concatenation of seven selected MLST fragments. The dendrogram shows the genetic relatedness among nonencapsulated strains.

biofilms. Interestingly, NESp strain 15P200 attached to the plate and formed a chain and clump and clustered to form a bacterial mass (Fig. 3A–C) along with mature biofilm formation (Fig. 3C). Conversely, 15P255 (serotype 24F), a low-level MBA-encapsulated strain (Fig. S1B), failed to form a biofilm and existed in single, independent, planktonic form (Fig. 3D and E).

Table 4
Antimicrobial susceptibility testing and detection of drug-resistance genes.

| Strain	ST	Mutation in PBP genes[a]	Presence of macrolide resistant genes[b]		Mutation in QRDR[c]				MIC (mg/L)							
			erm(B)	mef(A)	ParC	ParE	GyrA	GyrB	PEN	CTX	IPM	CLR	CLI	VAN	TFX	LVX
15P223*	7786	pbp2x	+	−	none	I460V	none	none	≤0.06	0.12	≤0.06	0.25	≤0.06	0.25	≤0.12	1
15P245*	7786	pbp2x	+	−	none	I460V	none	none	≤0.06	0.12	≤0.06	0.12	≤0.06	0.25	≤0.12	0.5
15P246	7786	pbp2x	+	−	none	I460V	none	none	≤0.06	0.12	≤0.06	0.12	≤0.06	0.25	≤0.12	0.5
15P232	11975	pbp1a + 2x + 2b	+	−	none	I460V	none	none	≤0.06	≤0.06	≤0.06	0.12	0.12	≤0.12	≤0.12	0.25
15P235	11975	pbp1a + 2x + 2b	+	−	none	I460V	none	none	≤0.06	≤0.06	≤0.06	0.5	8	≤0.12	≤0.12	0.5
15P237	11975	pbp1a + 2x + 2b	+	−	none	I460V	none	none	≤0.06	≤0.06	≤0.06	≤0.06	≤0.06	≤0.12	≤0.12	1
15P286	7502	pbp1a + 2x + 2b	+	−	none	I460V	none	none	0.25	0.12	≤0.06	>8	>8	0.25	≤0.12	1
15P303	7502	pbp1a + 2x + 2b	+	−	none	I460V	none	none	0.12	0.12	≤0.06	>8	>8	0.25	≤0.12	1
15P281	11976	pbp2x	+	−	none	I460V	none	none	≤0.06	≤0.06	≤0.06	0.25	≤0.06	0.25	≤0.2	0.5
15P291[d]	11976	pbp2x	+	−	none	I460V	none	none	≤0.06	0.25	≤0.06	>8	>8	0.25	≤0.12	1
15P292[d]	11976	pbp2x	+	−	none	I460V	none	none	≤0.06	0.25	≤0.06	>8	>8	0.50	≤0.12	1
15P293[d]	11976	pbp2x	+	−	none	I460V	none	none	≤0.06	0.12	≤0.06	>8	>8	0.25	≤0.12	1
15P192**	11973	pbp2x	+	−	K137 N	none	none	none	0.25	0.25	≤0.06	2	>8	0.25	≤0.12	1
15P195***	11974	pbp2x + 2b	+	−	K137 N	I460V	none	none	≤0.06	0.12	≤0.06	>8	>8	0.25	≤0.12	1
15P196	11974	pbp2x + 2b	+	−	K137 N	I460V	none	none	≤0.06	0.25	≤0.06	>8	>8	0.25	≤0.12	1
15P200**	11973	pbp2x	+	−	K137 N	none	none	none	0.25	0.25	≤0.06	1	>8	0.25	≤0.12	1
15P203***	11974	pbp2x + 2b	+	−	K137 N	I460V	none	none	≤0.06	0.25	≤0.06	>8	>8	0.25	≤0.12	1
15P205	11974	pbp2x + 2b	+	−	K137 N	I460V	none	none	≤0.06	0.12	≤0.06	8	>8	≤0.12	≤0.12	0.25

*, **, *** are isolated from the same child.

CLI, clindamycin; CLR, clarithromycin; CTX, cefotaxime; IPM, imipenem; LVX, levofloxacin; MIC, minimum inhibitory concentration; PBP, penicillin-binding protein; PEN, penicillin G; QRDR, quinolone-resistance-determining region; ST, sequence type; TFX, tosufloxacin; VAN, vancomycin.

[a] Mutations in penicillin-binding protein genes (pbp1a, 2x, and 2b), the targets of the β-lactams.

[b] The presence of the mef(A) and erm(B) genes was associated with resistance to macrolides; +, gene was detected; −, gene was not detected.

[c] The mutation in QRDR was associated with resistance to quinolones.

[d] Strains 15P291,15P292, and 15P293 were grown under 5% CO_2 because they could not grow under aerobic culture.
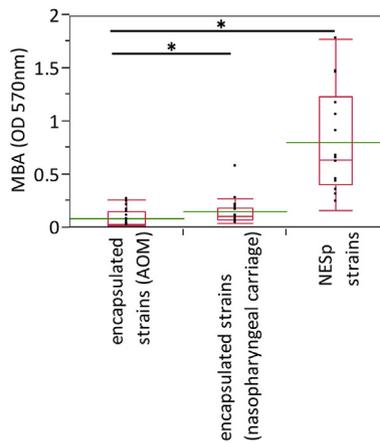
	Number of strains	Average biofilm formation	Standard deviation
encapsulated strains (AOM)	21	0.0705	0.0809
encapsulated strains (nasopharyngeal carriage)	19	0.1419	0.1217
NESp strains	18	0.7962	0.4898

Fig. 2. In vitro biofilm formation measured by a microtiter biofilm assay. Biofilm productivities of NESp strains, encapsulated strains isolated from nasopharyngeal carriage, and encapsulated strains isolated from otorrhea or middle-ear effusion with acute otitis media. Boxplot shows median and 10th, 25th, 75th, and 90th percentiles. Green lines show the average for each group. NESp strains tended to be more effective in generating biofilms than encapsulated strains, regardless of the source (*p < 0.001).

4. Discussion

This is the first report of bacterial characterization of NESp strains regarding their antibiotic susceptibility, possession of drug-resistance genes, and biofilm productivity. Nontypeable *S. pneumoniae* strains in AOM or carriage were reported from many countries after the introduction of PCV, especially PCV13; however, most reports identified nontypeable strains by the quellung reaction, thereby making it unclear whether these strains were true NESp. The prevalence of true NESp in the nasopharyngeal carriage of children has increased relative to that of encapsulated strains following the recent introduction of PCV in Portugal [4,23]. *PspK*-positive NESp was recently isolated from sinus cultures from children with chronic adenoiditis at adenoidectomy in the United States [24]. These strains are also found throughout several Asian countries and often isolated from the sputum, sinus aspirate, and middle ear [9]. In Japan, the rate of IPD caused by NESp is low (~0.2–0.3%) according to a population-based surveillance of pediatric IPD [1]. On the other hand, NESp was responsible for 4.7% and 9.5% of AOM and acute rhinosinusitis cases by *S. pneumoniae*, respectively [11]. Additionally, NESp was detected in 12.5% of nasopharyngeal samples from healthy children [11].

Here, the rate of NESp was also 12.0% (18/149) among healthy children in nursery school, which was consistent with previous reports [11]. All strains were *pspK*-positive and classified as NCC1, with the prevalence of these strains increasing annually in nursery school. The evaluation was difficult because the number of specimens was small in 2012, however, in 2013 and 2014, the total detection rates and the number of nursery schools detected NESp strains were clearly increased. There is a possibility that the prevalence of NESp strains is not only increasing in nursery schools but also in the entire region, and there is concern that it will increase further in the future. MLST analysis revealed that 5/18 (27.7%) of isolates were classified as either ST7502 or ST7786, which were previously reported in the Japanese MLST database [11]; however, these STs have not been identified in studies from other countries [7,9,24,25]. Notably, ST groupings tended to associate with specific nursery schools, indicative of horizontal spread. Furthermore, several strains were isolated from the same children at different time points. These data suggested that NESp could be a carriage occurring over several months.
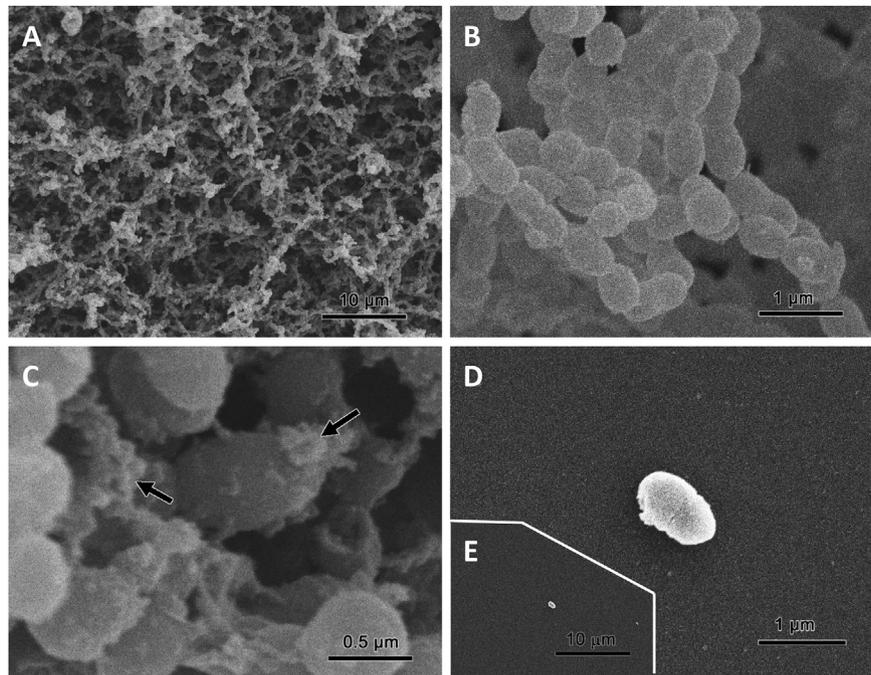
Fig. 3. Visualisation of biofilm morphology by SEM. (A−C) Strain 15P200 (NESp) was observed attaching to the plate and forming a chain and clump, and biofilms. The arrows show the biofilm structure. (D, E) Strain 15P255 (serotype 24F) was not observed forming a biofilm, but rather existed as a single, independent, and planktonic entity. NESp, nonencapsulated S. pneumoniae; SEM, scanning electron microscopy.

Molecular analysis of *pspK* demonstrated that the number of canonical repeat regions varied from 11 to 33 in our NESp isolates. A(E)EEAKR/QK is an α-helical structure with a highly charged LPXTG motif and a YPT motif that binds the human polymeric immunoglobulin receptor, which is an established epithelial pneumococcal receptor [7,26]. In the present study, several strains contained AEEEEAKRK or AEEEETKQK in novel repeat regions. Previous reports, mostly from Asian countries, indicated that strains often harbor from three to 38 repeats [7,9]. Interestingly, repeat variation is also observed between isolates belonging to the same ST, as well as between subsequent isolations from the same child. It is likely that these children might be consistently colonized, suggesting that this region is highly subject to genomic insertions or deletions.

Antimicrobial susceptibilities of NESp in our study indicated that all NESp isolates showed susceptibility to IPM and TFX; however, 22.2% (4/18) of the strains showed reduced susceptibility to PEN (0.12−0.25 mg/L). Furthermore, all NESp strains possessed at least one mutation in a PBP. Mutations in *pbp1a*, *pbp2b*, and *pbp2x* play important roles in the development of resistance to PEN and cephalosporin by *S. pneumoniae.* Specifically, this includes 9/18 (50.0%) strains harboring mutated *pbp2x*, 5/18 (27.8%) strains harboring mutated *pbp1a* + *pbp2x* + *pbp2b*, and 4/18 (22.2%) strains harboring mutated *pbp2x* + *pbp2b*. In terms of macrolide resistance, 11/18 (61.1%) strains were clarithromycin-resistant ($\geq$1 mg/L). Several strains were not grown in ambient air, therefore, these strains were cultured under 5% CO_2. A previous study showed that the MICs of macrolides and ketolides for *S. pneumoniae* under CO_2 tended to be 1- or 2-fold dilutions higher than those under ambient air due to lower pH [27]. All strains were positive for the macrolide-resistant *erm*(B) gene. In terms of quinolone resistance, 6/18 (33.3%) strains harbored a Lys137→Asn mutation in ParC, 16/18 (88.9%) strains harbored an Ile460→Val in ParE, and there were no strains with mutations in GyrA or GyrB. Resistance to fluoroquinolones in *S. pneumoniae* usually occurs by a stepwise process [28]. Low-level

quinolone resistance is caused by mutations in the QRDR of one of the subunits, with resistance progressing to a high level via additional mutations in the QRDR of the second target. Mutations in Ser81 in GyrA, Ser79 in ParC, or Asp83 in ParC are major mutations previously reported in quinolone-resistant *S. pneumoniae* [29]; however, these mutations were not found in this study. Mutations at Lys137→Asn in ParC and Ile460→Val in ParE are not known to contribute to fluoroquinolone resistance generally, but there is a report suggesting that the Lys137→Asn mutation in ParC affects the primary step in the development of high-level quinolone resistance [30,31]. No strains found in this study harbored mutations in both the QRDRs of *gyrA* and *parC*.

The prevalence of penicillin-resistant *S. pneumoniae* (PRSP) strains, such as serotypes 6B and 19F, decreased after PCV7, whereas serotypes 19A and 15A increased. After replacement with PCV13, serotype 19A strains decreased, but increases were observed in serotype 15A and 35B, which were not targeted by PCV13 and became problematic as drug-resistant strains [1,32−34]. NESp is also capable of becoming a drug-resistant serotype; therefore, it critical to continue monitoring drug susceptibility in NESp strains.

Because of its simplicity, requiring the use of basic laboratory materials, the microtiter plate assay is widely used as the method for studying biofilm formation. This assay tests the ability of bacteria to adhere to the plastic surface of a microtiter plate; crystal violet is used to stain the biofilm. Findings made by using microtiter plate assays should be confirmed by microscopy or another method. SEM is frequently used to observe the detailed structure of biofilms at the nanometer-scale level, but live biofilms cannot be observed by SEM. Biofilm observation methods employing fluorescent imaging methods that use confocal laser scanning microscopy and fluorescent protein expression systems have become the mainstream in biofilm studies for real time imaging of biofilms [35].

There are few studies regarding *S. pneumoniae* biofilm formation [36−38]; however, biofilm production in NESp strains has not

been investigated previously. The presence of capsules hinders biofilm development [37]. Consistently, nontypeable *Haemophilus influenzae* strains were more effective at generating biofilms than their encapsulated type b counterparts [39]. In the present study, NESp strains were more effective at forming biofilms than encapsulated strains, independent of the isolation source (e.g., carriage or AOM). Moreover, MBA analysis of MNZ1131 (Δ*pspK*) suggested that the presence of *pspK* did not affect the MBA, which can be an issue with encapsulated stains. Furthermore, SEM imaging revealed an obvious difference in the biofilms produced by NESp versus capsuled strain. Biofilms prevent neutrophil phagocytosis, inhibit the efficacy of antimicrobial agents, and lead to refractory infection. NESp represent a potential causative agents of chronic/recurrent otitis media, as shown using the chinchilla model [40]; therefore, biofilm production by NESp might relate to chronic/recurrent otitis media.

There are several limitations of this study. First, the NESp strains were isolated from the nasopharyngeal carriage of healthy children and not patients with infections; therefore, the characterized strains might not be clinically relevant. Additionally, samples were collected from a limited area, irrespective of population, which might limit their widespread application. Furthermore, the pathogenicity of the strains such as complement sensitivity was not evaluated. Further studies are needed in order to reveal the pathogenicity of NESp.

In conclusion, our study identified that the rate of NESp from nasopharyngeal carriage in healthy children was >10%. Many NESp strains were detected as drug resistant through the presence of genetic mutations, and biofilm production was substantially greater than that observed in encapsulated strains. These results suggested that infections due to NESp might represent an important clinical issue in the near future. Therefore, monitoring and investigation of the pathogenicity and drug sensitivity of NESp are extremely important for the development of treatment and prevention strategies.

Conflicts of interest

Ethical approval

This study was approved by the Ethical Committee of Medical Mycology Research Center, Chiba University (Permission No. 2017—12).

Funding

Acknowledgments

Appendix A. Supplementary data

Supplementary data to this article can be found online at https://doi.org/10.1016/j.jiac.2019.02.007.

References

[1] Suga S, Chang B, Asada K, Akeda H, Nishi J, Okada K, et al. Nationwide population-based surveillance of invasive pneumococcal disease in Japanese children: effects of the seven-valent pneumococcal conjugate vaccine. Vaccine 2015;33:6054—60.

[2] Bruce MG, Singleton R, Bulkow L, Rudolph K, Zulz T, Gounder P, et al. Impact of the 13-valent pneumococcal conjugate vaccine (pcv13) on invasive pneumococcal disease and carriage in Alaska. Vaccine 2015;33:4813—9.

[3] Isaacman DJ, McIntosh ED, Reinert RR. Burden of invasive pneumococcal disease and serotype distribution among *Streptococcus pneumoniae* isolates in young children in Europe: impact of the 7-valentpneumococcalconjugatevaccine and considerations for future conjugate vaccines. Int J Infect Dis 2010;14:e197—209.

[4] Nunes S, Félix S, Valente C, Simões AS, Tavares DA, Almeida ST, et al. The impact of private use of PCV7 in 2009 and 2010 on serotypes and antimicrobial resistance of *Streptococcus pneumoniae* carried by young children in Portugal: comparison with data obtained since 1996 generating a 15-year study prior to PCV13 introduction. Vaccine 2016;34:1648—56.

[5] Melchiorre S, Camilli R, Pietrantoni A, Moschioni M, Berti F, Del Grosso M, et al. Point mutations in *wchA* are responsible for the non-typability of two invasive *Streptococcus pneumoniae* isolates. Microbiology 2012;158:338—44.

[6] Park IH, Geno KA, Sherwood LK, Nahm MH, Beall B. Population-based analysis of invasive nontypeable pneumococci reveals that most have defective capsule synthesis genes. PLoS One 2014;9:e97825.

[7] Park IH, Kim KH, Andrade AL, Briles DE, McDaniel LS, Nahm MH. Nontypeable pneumococci can be divided into multiple *cps* types, including one type expressing the novel gene *pspK*. mBio 2012;3. e00035—12.

[8] Salter SJ, Hinds J, Gould KA, Lambertsen L, Hanage WP, Antonio M, et al. Variation at the capsule locus, cps, of mistyped and non-typable *Streptococcus pneumoniae* isolates. Microbiology 2012;158:1560—9.

[9] Na IY, Baek JY, Park IH, Kim DH, Song JH, Ko KS. *PspK* gene prevalence and characterization of non-typable *Streptococcus pneumoniae* isolates from Asian countries. Microbiology 2015;161:973—9.

[10] Keller LE, Friley J, Dixit C, Nahm MH, McDaniel LS. Nonencapsulated *Streptococcus pneumoniae* cause acute otitis media in the chinchilla that is enhanced by pneumococcal surface protein K. Open Forum Infect Dis 2014. https://doi.org/10.1093/ofid/ofu037.

[11] Hotomi M, Nakajima K, Hiraoka M, Nahm MH, Yamanaka N. Molecular epidemiology of nonencapsulated *Streptococcus pneumoniae* among Japanese children with acute otitis media. J Infect Chemother 2016;22:72—7.

[12] Berrón S, Fenoll A, Ortega M, Arellano N, Casal J. Analysis of the genetic structure of nontypeable pneumococcal strains isolated from conjunctiva. J Clin Microbiol 2005;43:1694—8.

[13] Shayegani M, Parsons LM, Gibbons Jr WE, Campbell D. Characterization of nontypable *Streptococcus pneumoniae*-like organisms isolated from outbreaks of conjunctivitis. J Clin Microbiol 1982;16:8—14.

[14] Pease AA, Douglas CW, Spencer RC. Identifying non-capsule strains of *Streptococcus pneumoniae* isolated from eyes. J Clin Pathol 1986;39:871—5.

[15] da Gloria Carvalho M, Pimenta FC, Jackson D, Roundtree A, Ahmad Y, Millar EV, et al. Revisiting pneumococcal carriage by use of broth enrichment and PCR techniques for enhanced detection of carriage and serotypes. J Clin Microbiol 2010;48:1611—8.

[16] Ehara N, Fukushima K, Kakeya H, Mukae H, Akamatsu S, Kageyama A, et al. A novel method for rapid detection of *Streptococcus pneumoniae* antigen in sputum and its application in adult respiratory tract infections. J Med Microbiol 2008;57:820—6.

[17] Fukushima K, Kubo T, Ehara N, Nakano R, Matsutake T, Ishimatu Y, et al. A novel method for rapid detection of *Streptococcus pneumoniae* antigens in blood. J Infect Chemother 2016;22:143—8.

[18] Enright MC, Spratt BG. A multilocus sequence typing scheme for *Streptococcus pneumoniae*: identification of clones associated with serious invasive disease. Microbiology 1998;144:3049—60.

[19] Japanese Society of Chemotherapy. Jpn J Chemother 2009;57:343—5. Japanese. Available at: http://www.chemotherapy.or.jp/guideline/breakpoint_respiratory.pdf. [Accessed 28 December 2018].

[20] Takeuchi N, Ohkusu M, Hoshino T, Naito S, Takaya A, Yamamoto T, et al. Emergence of quinolone-resistant strains in *Streptococcus pneumoniae* isolated from paediatric patients since the approval of oral fluoroquinolones in Japan. J Infect Chemother 2017;23:218—23.

[21] Keller LE, Luo X, Thornton JA, Seo KS, Moon BY, Robinson DA, et al. Immunization with pneumococcal surface protein K of nonencapsulated *Streptococcus pneumoniae* provides protection in a mouse model of colonization. Clin Vaccine Immunol 2015;22:1146—53.

[22] Namiki Y, Ueno K, Mitani H, Virtudazo EV, Ohkusu M, Shimizu K, et al. Scanning and negative-staining electron microscopy of protoplast regeneration of a wild-type and two chitin synthase mutants in the pathogenic yeast *Candida glabrata*. J Electron Microsc 2011;60:157—65.

[23] Sá-Leão R, Pinto F, Aguiar S, Nunes S, Carriço JA, Frazão N, et al. Analysis of invasiveness of pneumococcal serotypes and clones circulating in Portugal before widespread use of conjugate vaccines reveals heterogeneous behavior of clones expressing the same serotype. J Clin Microbiol 2011;49:1369—75.

[24] Dixit C, Keller LE, Bradshaw JL, Robinson DA, Swiatlo E, McDaniel LS. Nonencapsulated *Streptococcus pneumoniae* as a cause of chronic adenoiditis 2016;4:56—8. IDCases.

[25] Scott JR, Hinds J, Gould KA, Millar EV, Reid R, Santosham M, et al. Nontypeable pneumococcal isolates among Navajo and white mountain Apache communities: are these really a cause of invasive disease? J Infect Dis 2012;206:73–80.

[26] Zhang JR, Mostov KE, Lamm ME, Nanno M, Shimida S, Ohwaki M, et al. The polymeric immunoglobulin receptor translocates pneumococci across human nasopharyngeal epithelial cells. Cell 2000;102:827–37.

[27] Humphries RH, Hindler JA. Susceptibility test methods: fastidious bacteria. In: Jorgensen JH, Pfaller MA, Carroll KC, Funke G, Landry ML, Richter SS, et al., editors. Manual of clinical microbiology. 11th ed. Washington: American Society for Microbiology; 2015. p. 1314–41.

[28] Muñoz R, De La Campa AG. ParC subunit of DNA topoisomerase IV of *Streptococcus pneumoniae* is a primary target of fluoroquinolones and cooperates with DNA gyrase A subunit in forming resistance phenotype. Antimicrob Agents Chemother 1996;40:2252–7.

[29] Pan XS, Fisher LM. Cloning and characterization of the *parC* and *parE* genes of *Streptococcus pneumoniae* encoding DNA topoisomerase IV: role in fluoroquinolone resistance. J Bacteriol 1996;178:4060–9.

[30] Davies TA, Goldschmidt R, Pfleger S, Loeloff M, Bush K, Sahm DF, et al. Cross-resistance, relatedness and allele analysis of fluoroquinolone-resistant US clinical isolates of *Streptococcus pneumoniae* (1998-2000). J Antimicrob Chemother 2003;52:168–75.

[31] Oh WS, Suh JY, Song JH, Ko KS, Jung SI, Peck KR, et al. Fluoroquinolone resistance in clinical isolates of *Streptococcus pneumoniae* from Asian countries: ANSORP study. Microb Drug Resist 2004;10:37–42.

[32] Ubukata K, Chiba N, Hanada S, Morozumi M, Wajima T, Shouji M, et al. Invasive Pneumococcal Diseases Surveillance Study Group. Serotype changes and drug resistance in invasive pneumococcal diseases in adults after vaccinations in children, Japan, 2010-2013. Emerg Infect Dis 2015;21:1956–65.

[33] Varon E, Cohen R, Béchet S, Doit C, Levy C. Invasive disease potential of pneumococci before and after the 13-valent pneumococcal conjugate vaccine implementation in children. Vaccine 2015;33:6178–85.

[34] Angoulvant F, Cohen R, Doit C, Elbez A, Werner A, Béchet S, et al. Trends in antibiotic resistance of *Streptococcus pneumoniae* and *Haemophilus influenzae* isolated from nasopharyngeal flora in children with acute otitis media in France before and after 13 valent pneumococcal conjugate vaccine introduction. BMC Infect Dis 2015. https://doi.org/10.1186/s12879–015–0978–9.

[35] Cuevas RA, Eutsey R, Kadam A, West-Roberts JA, Woolford CA, Mitchell AP, et al. A novel streptococcal cell-cell communication peptide promotes pneumococcal virulence and biofilm formation. Mol Microbiol 2017;105:554–71.

[36] Allegrucci M, Sauer K. Characterization of colony morphology variants isolated from *Streptococcus pneumoniae* biofilms. J Bacteriol 2007;189:2030–8.

[37] Moscoso M, García E, López R. Biofilm formation by *Streptococcus pneumoniae*: role of choline, extracellular DNA, and capsular polysaccharide in microbial accretion. J Bacteriol 2006;188:7785–95.

[38] Hiller NL, Ahmed A, Powell E, Martin DP, Eutsey R, Earl J, et al. Generation of genetic diversity among *Streptococcus pneumoniae* strains via horizontal gene transfer during a chronic polyclonal pediatric infection. PLoS Pathog 2010;6: e1001108.

[39] Qin L, Kida Y, Ishiwada N, Ohkusu K, Kaji C, Sakai Y, et al. The relationship between biofilm formations and capsule in *Haemophilus influenzae*. J Infect Chemother 2014;20:151–6.

[40] Murrah KA, Pang B, Richardson S, Perez A, Reimche J, King L, et al. Nonencapsulated *Streptococcus pneumoniae* causes otitis media during single-species infection and during polymicrobial infection with nontypeable *Haemophilus influenzae*. Pathog Dis 2015. https://doi.org/10.1093/femspd/ftu011.